

Cite as: C. A. Neal *et al.*, *Science*
10.1126/science.aav7046 (2018).

The 2018 rift eruption and summit collapse of Kīlauea Volcano

C. A. Neal^{1*}, S.R. Brantley¹, L. Antolik¹, J. Babb¹, M. Burgess¹, K. Calles¹, M. Cappos¹, J. C. Chang¹, S. Conway¹, L. Desmither¹, P. Dotray¹, T. Elias¹, P. Fukunaga¹, S. Fuke¹, I. A. Johanson¹, K. Kamibayashi¹, J. Kauahikaua¹, R. L. Lee¹, S. Pekalib¹, A. Miklius¹, W. Million¹, C. J. Moniz¹, P. A. Nadeau¹, P. Okubo¹, C. Parcheta¹, M. P. Patrick¹, B. Shiro¹, D. A. Swanson¹, W. Tollett¹, F. Trusdell¹, E. F. Younger¹, M. H. Zoeller², E. K. Montgomery-Brown^{3*}, K. R. Anderson³, M. P. Poland⁴, J. Ball³, J. Bard⁵, M. Coombs⁶, H. R. Dietterich⁶, C. Kern⁵, W. A. Thelen⁵, P. F. Cervelli⁶, T. Orr⁶, B. F. Houghton⁷, C. Gansecki⁸, R. Hazlett⁸, P. Lundgren⁹, A. K. Diefenbach⁵, A. H. Lerner¹⁰, G. Waite¹¹, P. Kelly⁵, L. Clor⁵, C. Werner¹², K. Mulliken¹³, G. Fisher¹⁴

¹U.S. Geological Survey, Hawaiian Volcano Observatory, 51 Crater Rim Dr., Hawai'i National Park, Hawaii, HI 96718, USA. ²Center for the Study of Active Volcanoes, University of Hawai'i at Hilo, 200 W. Kāwili St., Hilo, HI 96720, USA. ³U.S. Geological Survey, California Volcano Observatory, 345 Middlefield Rd., Menlo Park, CA 94025, USA. ⁴U.S. Geological Survey, Yellowstone Volcano Observatory, 1300 SE Cardinal Ct., Suite 100, Vancouver, WA 98683-9589, USA. ⁵U.S. Geological Survey, Cascades Volcano Observatory, 1300 SE Cardinal Ct., Suite 100, Vancouver, WA 98683-9589, USA. ⁶U.S. Geological Survey, Alaska Volcano Observatory, 4230 University Dr., Anchorage, AK 99508, USA. ⁷Department of Earth Sciences, University of Hawai'i at Manoa, 1680 East-West Rd., Honolulu, HI 96822, USA. ⁸Geology Department, University of Hawai'i at Hilo, 200 W. Kāwili St., Hilo, HI 96720, USA. ⁹Jet Propulsion Laboratory, California Institute of Technology, 4800 Oak Grove Dr., Pasadena, CA 91109, USA. ¹⁰Department of Earth Sciences, University of Oregon, 100 Cascades Hall, Eugene, OR 97403, USA. ¹¹Department of Geological and Mining Engineering and Sciences, Michigan Technological University, 630 Dow Environmental Sciences, 1400 Townsend Dr., Houghton, MI 49931, USA. ¹²U.S. Geological Survey Contractor, 392 Tukapa St., RD1, New Plymouth 4371, New Zealand. ¹³State of Alaska Division of Geological and Geophysical Surveys, Alaska Volcano Observatory, 3354 College Rd., Fairbanks, AK 99709, USA. ¹⁴U.S. Geological Survey, National Civil Applications Center, 12201 Sunrise Valley Dr., MS-562, Reston, VA 20192, USA.

*Corresponding author. Email: tneal@usgs.gov (C.A.N.); emontgomery-brown@usgs.gov (E.K.M.-B.)

In 2018, Kīlauea Volcano experienced its largest lower East Rift Zone (LERZ) eruption and caldera collapse in at least 200 years. After collapse of the Pu'u 'Ō'ō vent on 30 April, magma propagated downrift. Eruptive fissures opened in the LERZ on 3 May, eventually extending ~6.8 km. A 4 May earthquake (M6.9) produced ~5 m of fault slip. Lava erupted at rates exceeding 100 m³/s, eventually covering 35.5 km². The summit magma system partially drained, producing minor explosions and near-daily collapses releasing energy equivalent to M4.7-M5.4 earthquakes. Activity declined rapidly on 4 August. Summit collapse and lava flow volume estimates are roughly equivalent—about 0.8 km³. Careful historical observation and monitoring of Kīlauea enabled successful forecasting of hazardous events.

Volcanic eruptions at basaltic shield volcanoes can threaten communities and infrastructure with a variety of hazards including lava flows, gas emissions, explosions and tephra fall, as well as damaging seismicity, ground collapse, and tsunamis. Eruption impacts can become global if sufficient ash or gas are transported through the atmosphere or if ocean-crossing tsunamis are generated. The 2018 eruption of Kīlauea Volcano in Hawai'i included both a summit caldera collapse and a flank fissure eruption, a complex event observed only a handful of times in modern history. Other large and well-documented caldera-forming eruptions at basaltic systems worldwide have been partially obscured [e.g., Bárðarbunga in Iceland, which collapsed in 2014–2015, is covered by a glacier; (1, 2)] or occurred over periods of hours to a few days [e.g., Fernandina 1968, Miyakejima 2000, and Piton de la Fournaise 2007; (3, 4, 5)]. Thanks to excellent accessibility and a dense network of geological, geochemical, and geophysical instrumentation, large data sets from the 2018 events at Kīlauea will prompt new scientific understanding of, for example, how calderas collapse and how caldera-rift zone systems

interact. In addition, the eruption and emergency response underscore the value of long-term observations to the science of volcanology and to risk mitigation.

Build up to 2018 activity

Kīlauea Volcano (Fig. 1), on the southeast side of the Island of Hawai'i, is supplied with mantle-derived magma that enters the shallow magma plumbing system below the summit caldera. Summit area magma can be stored, erupted, or transported laterally at shallow depth (~3 km) up to tens of kilometers along the volcano's rift zones—long, narrow areas of persistent eruption that are a hallmark of shield volcanoes. Prior to 30 April, 2018, Kīlauea had been erupting from two vents: (i) a lava lake within Halema'uma'u crater at the summit, active since 2008 (6), and (ii) Pu'u 'Ō'ō cone and nearby vents in the East Rift Zone (ERZ, Fig. 1), ~20 km from the summit, active since 1983 (7–9). The summit lava lake was characterized by emission of gas and small amounts of ash, while the ERZ eruption produced ~4.4 km³ of lava over 35 years [updated from (9)].

In mid-March 2018, tiltmeters at Pu‘u ‘Ō‘ō began to record inflationary ground deformation that was probably due to accumulation of magma. Previous episodes of pressurization at Pu‘u ‘Ō‘ō resulted in the formation of new eruptive vents within a few kilometers of the vent, for example in 2007 (10), 2011 (9), and 2014 (11). The pressure increase continued through March and April, causing the lava pond at Pu‘u ‘Ō‘ō to rise and prompting the Hawaiian Volcano Observatory (HVO) to issue a warning on 17 April that a new vent might form “either on the Pu‘u ‘Ō‘ō cone or along adjacent areas of the East Rift Zone.” The pressure increase eventually impacted the entire magma plumbing system, causing the summit lava lake to rise and ultimately overflow onto the floor of Halema‘uma‘u crater on 21 April, with another hazard notice issued by HVO on 24 April.

Lower East Rift Zone eruption

At 2:15 PM HST on 30 April (Fig. 2), geophysical data began indicating rapid changes occurring in the middle East Rift Zone (MERZ) magma system. Collapse of the Pu‘u ‘Ō‘ō crater floor was followed by ground deformation and eastward-propagating seismicity that indicated downrift intrusion of a dike toward the populated lower East Rift Zone (LERZ). On 1 May, HVO issued a warning to residents downrift that an eruption was possible. Seismicity and ground deformation provided indications of extensional deformation associated with a magmatic intrusion. Ground deformation was measured with borehole tiltmeters, real-time Global Navigation Satellite System (GNSS), and satellite interferometric synthetic aperture radar (InSAR), the latter of which included an acquisition by the European Space Agency’s Sentinel-1 satellite on 2 May. These data indicated that the intrusion was approaching the Leilani Estates subdivision, about 20 km downrift from Pu‘u ‘Ō‘ō. The first of 24 eruptive fissures opened within the subdivision just before 5:00 PM HST on 3 May.

The eruptive fissures that formed during the first week of the LERZ eruption were up to several hundred meters long and generally short-lived (minutes to hours), with spatter and lava accumulating within a few tens of meters of individual vents. The sluggish lava was of a composition (≤ 5 wt.% MgO) that suggested long-term storage prior to eruption. It was also chemically similar to lava erupted in the same area in 1955 (12), implying that the magma had been stored in the rift for decades.

On 4 May, the largest (Mw 6.9) earthquake on the island in 43 years occurred beneath Kīlauea’s south flank at a depth of ~6 km based on seismic data (Fig. 3). Focal mechanism analysis suggests that the earthquake was probably located on the sub-horizontal basal décollement fault between the volcanic pile and the preexisting seafloor (13). Ground deformation models indicate up to ~5 m of seaward fault slip (Fig.

3) based on up to 0.7 m of coseismic seaward displacement at GNSS stations. The aftershock pattern was consistent with our geodetic model, with a slip patch extending 25 km offshore and spanning an area of about 700 km². The earthquake may have been motivated by the dike intrusion—a hypothesis that is supported by stress models showing that rift zone opening promotes décollement fault failure (14, 15). Earthquakes (usually in the M4-5 range) have also occurred during and immediately following past Kīlauea ERZ intrusions [e.g., 2007 Father’s Day intrusion, (10)].

We modeled ALOS-2 and Sentinel-1 interferograms spanning the first few days of the LERZ eruption and found contraction along much of the MERZ along with up to ~4 m of subsurface opening in the LERZ (Fig. 3). Following the onset of eruption, we found evidence of downrift propagation of the intrusion from earthquake activity and deformation, although no new fissures or cracks opened on 10 or 11 May. On 10 May, HVO issued a status report suggesting that more lava outbreaks were likely, and on 12 May a new fissure opened 1.6 km downrift of the previous eruptive activity in a location where earthquakes had clustered in the previous two days. On 18 May, hotter and less viscous lava began erupting (movie S1), resulting in long, fast-moving lava flows that reached the ocean on the southeast side of the island five days later. This change in eruptive character provided an indication, supported by changes in chemical composition, that “fresh” magma derived from the summit and MERZ was now beginning to erupt from the LERZ fissures.

To assess changing lava hazards to now-threatened surrounding communities, HVO produced rapid preliminary lava flow path forecasts based on steepest descent path modeling [Fig. 4; (11, 16, 17)]. Throughout the eruption, lava flow path simulations that utilized updated topography were run from active flow fronts, new fissures, and channel overflow locations, yielding maps of likely future flow directions (Fig. 4).

Eruptive activity resumed at fissure 8, in east-central Leilani Estates, late on 27 May (Fig. 4), and activity became focused there within 12 hours, on 28 May. Lava fountains reached heights of 80 m and fed a rapid channelized flow that ultimately entered the ocean near the eastern tip of the island (following potential routes indicated in the initial forecast, Fig. 4). SO₂ emissions climbed to more than 50,000 tonnes per day, severely impacting air quality across the island and reaching as far as Guam (>6000 km). Estimated effusion rates ranged from 50–200 m³/s (dense-rock equivalent) during this part of the eruption. Effusion of large amounts of lava ended abruptly on 4 Aug 2018. Based on a combination of topographic differences and fissure 8 vent flux over time, we estimate a preliminary erupted volume of ~0.8 to possibly greater than 1 km³ of lava. The volume of the 2018 intruded dike (Fig. 3C and fig. S2) is approximately 10% of the erupted volume.

Summit collapse

Summit subsidence and lava lake withdrawal began gradually on 1 May and accelerated in the days following the M6.9 earthquake (Fig. 2). The summit lava lake level, which in previous years rose and fell in concert with summit deformation and adjustments in vent elevation of Pu‘u ‘Ō‘ō (18), dropped over 300 m and was no longer visible from the crater rim by 10 May. In 1924, a substantial drop in lava level associated with a LERZ intrusion was followed by explosive activity that included ash emissions and ejection of blocks onto the caldera floor (19). The hypothesis for the 1924 explosions had been that they resulted from groundwater mixing with the hot rock of the recently evacuated magma conduit (20, 21). Based on this analogy, HVO issued a warning of “the potential for explosive eruptions in the coming weeks” on 9 May.

By 10 May, sporadic ejections of mixed juvenile and lithic ash reached heights of ~2000 m above the summit eruptive vent (e.g., Fig. 2), accompanied by hundreds of M3–4 summit earthquakes per day. Most of Hawai‘i Volcanoes National Park closed on 11 May due to the increase in seismicity and in anticipation of explosive activity. On 16 May, one day after HVO issued a notice of the potential for stronger explosions, the first of several small explosive events occurred, ejecting non-juvenile ash that was transported southwest by the wind while small (<1 m) ballistic blocks landed within a few hundred meters of the vent.

Minor explosions continued and slope failures widened the former eruptive vent that had contained the lava lake as summit deflation progressed through May. From 16 to 26 May, 12 explosions occurred at intervals of 8–45 hours. Each event was characterized by an inflationary tilt step, VLP seismic signals with moment magnitudes of M4.7–5.1, and a small amount of high-frequency shaking. Moment tensor inversions reveal a complex source process dominated by changes in volume rather than the slip on a planar fault that is typical of a tectonic earthquake. Plume heights from small explosions varied due to eruption intensity and atmospheric conditions, with the largest reaching about 8100 m above ground level on 17 May. Summit SO₂ emission rates increased by 2–3 times and peaked during this stage of explosive activity. This trend is not compatible with the groundwater origin for the source of the explosions and also calls into question the hypothesis put forth for the 1924 activity (20–22).

Starting near the end of May, the floor of Kīlauea caldera around Halema‘uma‘u crater began to subside as the walls of the crater slumped inward (movie S2). As the vent filled with rock-fall rubble, the background plume of ash from the vent greatly diminished, magmatic gas emissions decreased markedly, and ash eruption gradually slowed. A total of 62 collapse events occurred between May and early August. Seismic, infrasonic and geodetic signals settled into a remarkably consistent pattern characterized by M5.2–5.4 VLP collapse events

occurring almost daily, with intervening escalating earthquake swarms exceeding 700 \leq M4.0 earthquakes per day. During this phase, higher frequency seismic energy and strong infrasound signals accompanied the remarkably consistent VLP signal originally associated with explosions, and the caldera floor dropped several meters during each of the large events, ultimately deepening in places by over 500 m (Fig. 5). The persistent high levels of seismicity caused substantial damage to infrastructure in Hawai‘i Volcanoes National Park, including to the by-then-evacuated HVO facility.

The episodic subsidence of the caldera floor was likely driven by the nearly constant magma withdrawal from the summit reservoir system to feed the LERZ eruption (1–4). Starting in July, transient tilt signals were detected at down-rift instruments following summit collapse events, suggesting that the collapses were driving pressure increases that propagated down the East Rift Zone. Some of these pressure transients were followed by observations of increased effusion rate at the LERZ eruption site. The summit subsidence largely stopped by 4 August—about the same time as the end of major LERZ effusion—and the last collapse event occurred on 2 August. The 0.825 km³ volume of the collapse (based on topographic differences; Fig. 5) is similar to the volume of LERZ effusion.

Synthesis of 2018 activity

The 2018 activity at Kīlauea reflects changes in a well-connected magmatic plumbing system from the volcano’s summit to its lower flank (Fig. 6). The summit magmatic system consists of at least two magma storage areas, one centered about 1–2 km beneath the former east margin of Halema‘uma‘u crater and another larger one 3–5 km beneath the south part of the caldera [Fig. 6; (23)]. Deformation associated with the 2018 collapse suggests substantial drainage of the shallower reservoir.

Caldera collapses have been observed under challenging circumstances at only a few volcanoes worldwide [e.g., Miyakejima, Piton de la Fournaise, Fernandina, and Bárðarbunga; (1, 4, 5, 24)]. At Kīlauea, substantial, protracted, incremental caldera collapse occurred in the midst of a strong monitoring infrastructure, providing abundant opportunity for observation and investigation and helping to refine models of hazardous volcanic activity. As an example, the 1924 explosions were interpreted as due to the interaction of water with hot rock. The 2018 explosions of lithic ash were accompanied by heightened SO₂ emissions, suggesting the collapse and rockfalls may have agitated the magmatic system and released gas that entrained rockfall debris. These observations are not only a window into activity in 2018, but also will facilitate reinterpretation of past events.

The high effusion rate of the LERZ vents was sustained longer than that of any observed Kīlauea eruption. While past

eruptions have produced more total lava, the effusion rates were much lower, and the eruptions lasted for years to decades (7, 25–27). The voluminous 2018 eruptive activity probably was driven by a combination of factors, foremost among these being the pressurized pre-eruptive state of the summit and ERZ and the relatively low elevation of the eruptive vent. Past eruptions on the ERZ have demonstrated a correlation between the magnitude of total co-eruptive summit deflation and vent elevation, with the greatest summit deflation coinciding with the lowest-elevation vents (18, 28). The summit collapse, however, might also act as a mechanism to drive magma toward the rift zone, as suggested by the ERZ pressure pulses. Additionally, LERZ effusive surges were occurring, of which some in July followed collapse events at the summit. These observations reflect a complex feedback process between the LERZ eruptive vent and the summit collapse.

The initiation mechanism for the extraordinary 2018 LERZ eruption and summit collapse remains enigmatic. Previous episodes of inflation at Pu‘u ‘Ō‘ō resulted in the formation of new eruptive vents nearby, but not in the downrift transport of large amounts of magma. One explanation is that the initial rupturing of a barrier in the MERZ allowed substantial volumes of magma to move into the LERZ for the first time since 1960, and the highly pressurized state of the magmatic system probably facilitated downrift transport of magma from the summit. Long-term flank slip and deep ERZ opening promotes extension in the shallow rift [e.g., (29, 30)], so the LERZ was already primed for an intrusion by 2018, given that almost 60 years of extension had accumulated since the last intrusion. The 4 May M6.9 earthquake may have also aided magma transport (31), because décollement fault slip can result in rift zone opening [e.g., (32)]. The strong hydraulic connection between the summit and LERZ, once established, remained until the summit magmatic system drained to a point where the LERZ eruption could no longer be sustained.

The 4 May M6.9 earthquake marked an important event in the magmatic cycle of Kīlauea Volcano. Major flank slip events occur frequently on Kīlauea. A suggested cycle, in which the flank progressively stiffens as it nears the next flank earthquake, results in gradually increasing magmatic head and more frequent eruptive activity (33). Once the flank slips, the magmatic head drops, and eruptions become smaller and less frequent. The latest example of such a period occurred after the 1975 M7.7 Kalapana earthquake. Between that earthquake and the beginning on the Pu‘u ‘Ō‘ō eruption in 1983, only 3 small eruptive events occurred, although there were at least a dozen intrusive events (33).

The loss of magmatic head due to the earthquake, coupled with the evacuation of magma from the summit in 2018, suggests that it may take several years before enough magma can

accumulate beneath the summit to erupt. After the 1924 summit collapse, which may also have been associated with flank instability (33), only a few small eruptions confined to Halema‘uma‘u crater occurred in the ensuing 10 years, and there was a total absence of eruptions anywhere on the volcano for another 18 years. If future activity at Kīlauea follows a similar pattern, the next several years will see little, if any, significant eruptive activity. However, it is also possible that reduced summit magma pressure may promote higher rates of magma supply from depth due to a pressure imbalance between the deep and shallow parts of Kīlauea’s magma plumbing system [e.g., (34)], which could result in renewed eruptive activity sooner than expected. The next several years offer an exceptional and exciting opportunity to study the evolution of magmatism following a major perturbation to Kīlauea’s plumbing system.

Volcano observatory science and emerging technology

Since HVO’s founding in 1912, its scientists have committed to better understand how Hawaiian volcanoes work, decipher eruption histories, and improve strategies for responding to eruptions and issuing public hazard notifications. Indeed, HVO’s founder, Thomas Jaggar, held that earthquake and volcano processes must be studied not only after the event, but also before and during their occurrence. Only by such long-term study, he reasoned, could such processes be understood sufficiently to allow for effective risk reduction, including forecasting (35). The 2018 LERZ eruption and summit collapse of Kīlauea challenged HVO like never before to apply the lessons learned in over 100 years of study. Intensive observations of historical eruptions provided a framework (but not absolute constraints) for interpreting the activity and associated hazards (36–38). Eruptions in Kīlauea’s LERZ in 1955 and 1960 were both accompanied by large summit subsidence (although not to the degree of the current episode), and withdrawal of a lava lake in 1924 preceded explosions at the summit. This knowledge of Kīlauea’s geology was augmented by a comprehensive instrumental monitoring network of geological, geochemical, and geophysical sensors spread across the volcano and deployed in response to the unfolding eruption and summit collapse (Fig. 1).

This eruption also enabled the broader use of emerging technologies, such as the use of unoccupied aircraft systems (UAS), infrasound arrays, inexpensive webcam networks, real-time GNSS, multimedia communication systems, and alarm systems for automatic notification of specific parameters. For example, infrasonic alarms were developed to alert on changes in summit or rift zone eruption location or vigor, complementing existing seismic alarms. These were integrated into an enhanced real-time communication system (voice, text, images and video) which enabled transparent and instantaneous information transfer between field

observers and scientists monitoring data. On-demand lava flow path modeling (Fig. 4) based on topography updated during the eruption augmented steepest descent paths to identify changes in potential flow paths. SO₂ emission rates were continuously used to update air quality forecasts for the island, and gas compositions were tracked in non-evacuated areas along the fissure axis to monitor for potential signs of ascending magma. Rapid chemical and petrographic lava sample analysis provided information on changing magma compositions while the eruption progressed. Frequent UAS flights facilitated much of this work, for example, by enabling gas emission measurements and topographic data collection from areas that would not otherwise be accessible. Simultaneously, the geologic record guided thinking about potential outcomes of the eruption and collapse, including the size and type of summit explosions and the duration and volume of the LERZ eruption. These methods have the potential to be applied to aid in future eruption responses in Hawai'i and elsewhere.

Concluding remarks

The protracted 2018 summit collapse and flank eruption at Kīlauea provided an outstanding opportunity to observe and measure hazardous volcanic phenomena using an array of techniques with exceptional resolution in both space and time. These observations have already yielded new insights into poorly known processes such as caldera collapse, small-scale explosive basaltic volcanism, vigorous lava effusion and degassing, and magma transport and flank stability at shield volcanoes. Continued exploitation of these rich data sets will undoubtedly yield additional discoveries that will refine understanding of Kīlauea Volcano and volcanic processes and hazards in general. The success of HVO in detecting and, to the extent possible, forecasting various elements of the 2018 eruptive activity is a strong argument for continuous and intensive ground-based monitoring of geologic processes to inform hazards assessment and risk mitigation. Furthermore, the collective scientific response and lessons learned during this most recent Kīlauea eruption offer emphatic validation of Thomas Jaggar's vision for the role and value of a volcano observatory.

REFERENCES AND NOTES

1. F. Sigmundsson, A. Hooper, S. Hreinsdóttir, K. S. Vogfjörð, B. G. Ófeigsson, E. R. Heimisson, S. Dumont, M. Parks, K. Spaans, G. B. Gudmundsson, V. Drouin, T. Árnadóttir, K. Jónsdóttir, M. T. Gudmundsson, T. Högnadóttir, H. M. Fridriksdóttir, M. Hensch, P. Einarsson, E. Magnússon, S. Samsonov, B. Brandsdóttir, R. S. White, T. Ágústsdóttir, T. Greenfield, R. G. Green, Á. R. Hjartardóttir, R. Pedersen, R. A. Bennett, H. Geirsson, P. C. La Femina, H. Björnsson, F. Pálsson, E. Sturkell, C. J. Bean, M. Möllhoff, A. K. Braiden, E. P. S. Eibl, Segmented lateral dyke growth in a rifting event at Bárðarbunga volcanic system, Iceland. *Nature* **517**, 191–195 (2015). doi:10.1038/nature14111 Medline
2. M. T. Gudmundsson, K. Jónsdóttir, A. Hooper, E. P. Holohan, S. A. Halldórsson, B. G. Ófeigsson, S. Cesca, K. S. Vogfjörð, F. Sigmundsson, T. Högnadóttir, P. Einarsson, O. Sigmarrsson, A. H. Jarosch, K. Jónasson, E. Magnússon, S. Hreinsdóttir, M. Bagnardi, M. M. Parks, V. Hjörleifsdóttir, F. Pálsson, T. R. Walter, M. P. J. Schöpfer, S. Heimann, H. I. Reynolds, S. Dumont, E. Bali, G. H. Gudfinnsson, T. Dahm, M. J. Roberts, M. Hensch, J. M. C. Belart, K. Spaans, S. Jakobsson, G. B. Gudmundsson, H. M. Fridriksdóttir, V. Drouin, T. Dürig, G. Adalgeirsdóttir, M. S. Riishuus, G. B. M. Pedersen, T. van Boeckel, B. Oddsson, M. A. Pfeffer, S. Barsotti, B. Bergsson, A. Donovan, M. R. Burton, A. Aiuppa, Gradual caldera collapse at Bárðarbunga volcano, Iceland, regulated by lateral magma outflow. *Science* **353**, aaf8988 (2016). doi:10.1126/science.aaf8988 Medline
3. J. Filson, T. Simkin, L.-K. Leu, Seismicity of a caldera collapse: Galápagos Islands 1968. *J. Geophys. Res.* **78**, 8591–8622 (1973). doi:10.1029/JB078i035p08591
4. H. Kumagai, T. Ohminato, M. Nakano, M. Ooi, A. Kubo, H. Inoue, J. Oikawa, Very-long-period seismic signals and caldera formation at Miyake Island, Japan. *Science* **293**, 687–690 (2001). doi:10.1126/science.1062136 Medline
5. L. T. Michon, V. Staudacher, V. Ferrazzini, P. Bachèlery, J. Marti, April 2007 collapse of Piton de la Fournaise: A new example of caldera formation. *Geophys. Res. Lett.* **34**, L21301 (2007). doi:10.1029/2007GL031248
6. M. R. Patrick, T. R. Orr, D. A. Swanson, T. Elias, B. Shiro, "Lava lake activity at the summit of Kīlauea Volcano in 2016" (U.S. Geological Survey Scientific Investigations Report 2018–5008, USGS, 2018).
7. E. W. Wolfe, "The Pu'u 'Ō'ō eruption of Kīlauea Volcano, Hawaii: Episodes 1 through 20, January 3, 1983, through June 8, 1984" (U.S. Geological Survey Professional Paper 1463, USGS, 1988).
8. C. Heliker, T. N. Mattox, "The first two decades of the Pu'u 'Ō'ō-Kūpaianaha eruption: chronology and selected bibliography," in *The Pu'u 'Ō'ō-Kūpaianaha Eruption of Kīlauea Volcano, Hawai'i: The First 20 Years*, C. Heliker, D. A. Swanson, T. J. Takahashi, Eds. (U.S. Geological Survey Professional Paper 1676, USGS, 2003).
9. T. R. Orr, M. P. Poland, M. R. Patrick, W. A. Thelen, A. J. Sutton, T. Elias, C. R. Thornber, C. Parcheta, K. M. Wooten, "Kīlauea's 5–9 March 2011 Kamoamoā fissure eruption and its relation to 30+ years of activity From Pu'u 'Ō'ō," in *Hawaiian Volcanoes: From Source to Surface*, R. Carey, V. Cayol, M. P. Poland, D. Weis, Eds. (Geophysical Monograph Series, vol. 208, American Geophysical Union and Wiley, 2015), chap. 18, pp. 393–420.
10. M. P. Poland, A. Miklius, T. Orr, A. J. Sutton, C. R. Thornber, C. R. D. Wilson, New episodes of volcanism at Kīlauea Volcano, Hawaii. *Eos (Wash. D.C.)* **89**, 37–38 (2008). doi:10.1029/2008E0050001
11. M. P. Poland, T. R. Orr, J. P. Kauahikaua, S. R. Brantley, J. L. Babb, M. R. Patrick, C. A. Neal, K. R. Anderson, L. Antolik, M. Burgess, T. Elias, S. Fuke, P. Fukunaga, I. A. Johanson, M. Kagimoto, K. Kamibayashi, L. Lee, A. Miklius, W. Million, C. Moniz, P. G. Okubo, The 2014–2015 Pāhoā lava flow crisis at Kīlauea Volcano, Hawai'i: Disaster avoided and lessons learned. *GSA Today* **26**, 4–10 (2016).
12. R. A. Ho, M. O. Garcia, Origin of differentiated lavas at Kīlauea Volcano, Hawaii: Implications from the 1955 eruption. *Bull. Volcanol.* **50**, 35–46 (1988). doi:10.1007/BF01047507
13. D. P. Hill, Crustal structure of the island of Hawaii from seismic-refraction measurements. *Bull. Seismol. Soc. Am.* **59**, 101–130 (1969).
14. E. K. Desmarais, P. Segall, Transient deformation following the 30 January 1997 dike intrusion at Kīlauea volcano, Hawai'i. *Bull. Volcanol.* **69**, 353–363 (2007). doi:10.1007/s00445-006-0080-7
15. B. A. Brooks, J. Foster, D. Sandwell, C. J. Wolfe, P. Okubo, M. Poland, D. Myer, Magmatically triggered slow slip at Kīlauea volcano, Hawaii. *Science* **321**, 1177 (2008). doi:10.1126/science.1159007 Medline
16. J. P. Kauahikaua, T. Orr, M. R. Patrick, F. Trusdell, "Steepest-descent lines for Kīlauea, Mauna Loa, Hualālai, and Mauna Kea Volcanoes, Hawai'i" (U.S. Geological Survey Scientific Investigations Report 2016–5059, USGS, 2016).
17. M. Favalli, M. T. Pareschi, A. Neri, I. Isola, Forecasting lava flow paths by a stochastic approach. *Geophys. Res. Lett.* **32**, L03305 (2005).
18. M. R. Patrick, K. R. Anderson, M. P. Poland, T. R. Orr, D. A. Swanson, Lava lake level as a gauge of magma reservoir pressure and eruptive hazard. *Geology* **43**, 831–834 (2015). doi:10.1130/G36896.1
19. D. A. Swanson, T. R. Rose, A. E. Mucek, M. O. Garcia, R. S. Fiske, L. G. Mastin, Cycles of explosive and effusive eruptions at Kīlauea Volcano, Hawai'i. *Geology* **42**, 631–634 (2014). doi:10.1130/G35701.1
20. T. A. Jaggar, "Monthly Bulletin of the Hawaiian Volcano Observatory, vol. 12, no. 5 (May 1924)" reprinted in *The Early Serial Publications of the Hawaiian Volcano*

- Observatory, D. Bevens, T. J. Takahashi, T. L. Wright, Eds. (Hawaii Natural History Association, Hawaii National Park, Hawaii, 1988).
21. H. T. Stearns, The explosive phase of Kilauea Volcano, Hawaii, in 1924. *Bull. Volcanol.* **2**, 193–208 (1925). [doi:10.1007/BF02719505](https://doi.org/10.1007/BF02719505)
 22. R. W. Decker, R. L. Christiansen, "Explosive eruptions of Kilauea Volcano, Hawaii," in *Explosive Volcanism: Inception, Evolution, and Hazards* (Studies in Geophysics Series, National Academies Press, 1984), pp. 122–132.
 23. M. P. Poland, A. Miklius, E. K. Montgomery-Brown, "Magma supply, storage, and transport at shield-stage Hawaiian volcanoes," in *Characteristics of Hawaiian Volcanoes*, M. P. Poland, T. J. Takahashi, C. Landowski, Eds. (U.S. Geological Survey Professional Paper 1801, USGS, 2014), chap. 5.
 24. N. Geshi, T. Shimano, T. Chiba, S. Nakada, Caldera collapse during the 2000 eruption of Miyakejima Volcano, Japan. *Bull. Volcanol.* **64**, 55–68 (2002). [doi:10.1007/s00445-001-0184-z](https://doi.org/10.1007/s00445-001-0184-z)
 25. R. B. Moore, Volcanic geology and eruption frequency, lower east rift zone of Kilauea volcano, Hawaii. *Bull. Volcanol.* **54**, 475–483 (1992). [doi:10.1007/BF00301393](https://doi.org/10.1007/BF00301393)
 26. R. I. Tilling, Fluctuations in surface height of active lava lakes during 1972–1974 Mauna Ulu eruption, Kilauea volcano, Hawaii. *J. Geophys. Res.* **92**, 13721–13730 (1987). [doi:10.1029/JB092iB13p13721](https://doi.org/10.1029/JB092iB13p13721)
 27. D. A. Swanson, W. A. Duffield, D. B. Jackson, D. W. Peterson, "Chronological narrative of the 1969–71 Mauna Ulu eruption of Kilauea Volcano, Hawaii" (U.S. Geological Survey Professional Paper 1056, USGS, 1979).
 28. D. Epp, R. W. Decker, A. T. Okamura, Relation of summit deformation to East Rift Zone eruptions on Kilauea Volcano, Hawaii. *Geophys. Res. Lett.* **10**, 493–496 (1983). [doi:10.1029/GL010i007p00493](https://doi.org/10.1029/GL010i007p00493)
 29. P. T. Delaney, R. S. Fiske, A. Miklius, A. T. Okamura, M. K. Sako, Deep magma body beneath the summit and rift zones of Kilauea Volcano, Hawaii. *Science* **247**, 1311–1316 (1990). [doi:10.1126/science.247.4948.1311](https://doi.org/10.1126/science.247.4948.1311) [Medline](#)
 30. S. Owen, P. Segall, M. Lisowski, A. Miklius, M. Murray, M. Bevis, J. Foster, January 30, 1997 eruptive event on Kilauea Volcano, Hawaii, as monitored by continuous GPS. *Geophys. Res. Lett.* **27**, 2757–2760 (2000). [doi:10.1029/1999GL008454](https://doi.org/10.1029/1999GL008454)
 31. C. Liu, T. Lay, X. Xiong, Rupture in the 4 May 2018 MW6.9 earthquake seaward of the Kilauea East Rift Zone fissure eruption in Hawaii. *Geophys. Res. Lett.* **45**, 9508–9515 (2018). [doi:10.1029/2018GL079349](https://doi.org/10.1029/2018GL079349)
 32. E. K. Montgomery-Brown, M. P. Poland, A. Miklius, "Delicate balance of magmatic-tectonic interaction at Kilauea Volcano, Hawai'i, revealed from slow slip events," in *Hawaiian Volcanoes: From Source to Surface*, R. Carey, V. Cayol, M. P. Poland, D. Weis, Eds. (Geophysical Monograph Series, vol. 208, American Geophysical Union and Wiley, 2015), chap. 13, pp. 269–288.
 33. R. P. Denlinger, J. K. Morgan, "Instability of Hawaiian volcanoes" in *Characteristics of Hawaiian Volcanoes*, M. P. Poland, T. J. Takahashi, C. Landowski, Eds. (U.S. Geological Survey Professional Paper 1801, USGS, 2014), chap. 4.
 34. J. J. Dvorak, D. Dzurisin, Variations in magma supply rate at Kilauea Volcano, Hawaii. *J. Geophys. Res.* **98**, 22255–22268 (1983). [doi:10.1029/93JB02765](https://doi.org/10.1029/93JB02765)
 35. J. Kauahikaua, M. Poland, One hundred years of volcano monitoring in Hawaii. *Eos (Wash. D.C.)* **93**, 29 (2012). [doi:10.1029/2012EO030001](https://doi.org/10.1029/2012EO030001)
 36. U.S. Geological Survey Hawaiian Volcano Observatory, "Preliminary analysis of the ongoing Lower East Rift Zone (LERZ) eruption of Kilauea Volcano: Fissure 8 Prognosis and Ongoing Hazards" (Cooperator Report to Hawaii County Civil Defense, 15 July 2018); https://volcanoes.usgs.gov/vsc/file_mgrn/file-185/USGS%20Preliminary%20Analysis_LERZ_7-15-18_v1.1.pdf.
 37. U.S. Geological Survey Hawaiian Volcano Observatory, "Volcanic hazard at the summit of Kilauea: June 29, 2018 Update" (Report, 2018); https://volcanoes.usgs.gov/vsc/file_mgrn/file-184/Summit%20scenarios_7-5-18.pdf. **Error! Hyperlink reference not valid.**
 38. K. R. Anderson, D. A. Swanson, L. Mastin, C. Neal, B. F. Houghton, "Preliminary analysis of current explosion hazards at the summit of Kilauea Volcano" (Cooperator Report To: Hawai'i Volcanoes National Park, U.S. Geological Survey, 8 May 2018); https://volcanoes.usgs.gov/vsc/file_mgrn/file-180/PreliminaryAnalysisOfCurrentExplosionHazardsSummit_May8_2018.pdf.
 39. Hawaiian Volcano Observatory Staff, Preliminary map of the 2018 lower East Rift Zone eruption of Kilauea Volcano, Island of Hawai'i (U.S. Geological Survey, 2018); <https://www.sciencebase.gov/catalog/item/5afe0ba7e4b0da30c1bdb96db>.
 40. Incorporated Research Institutions for Seismology (IRIS), Data services; <https://ds.iris.edu/>.
 41. U.S. Geological Services, USGS comprehensive catalog; <https://earthquake.usgs.gov/>.
 42. European Space Agency Sentinel Data Access; <https://sentinel.esa.int/web/sentinel/sentinel-data-access>.
 43. GPS Solutions, RTNet software package; <https://gps-solutions.com/>.
 44. National Center for Airborne Laser Mapping (NCALM), Hawaii Big Island Survey Dataset, OpenTopography (2012); <http://dx.doi.org/10.5069/G9D7067X>.
 45. Kilauea LiDAR Data (2018); <https://kilauealidar.com/>.
 46. E. K. Montgomery-Brown, D. K. Sinnett, M. Poland, P. Segall, T. Orr, H. Zebker, A. Miklius, Geodetic evidence for an echelon dike emplacement and concurrent slow slip during the June 2007 intrusion and eruption at Kilauea volcano, Hawaii. *J. Geophys. Res. Solid Earth* **B7**, 115 (2010). [doi:10.1029/2009JB006658](https://doi.org/10.1029/2009JB006658)
 47. B. Galle, C. Oppenheimer, A. Geyer, A. J. S. McGonigle, M. Edmonds, L. Horrocks, A miniaturised ultraviolet spectrometer for remote sensing of SO₂ fluxes; a new tool for volcano surveillance. *J. Volcanol. Geotherm. Res.* **119**, 241–254 (2003). [doi:10.1016/S0377-0273\(02\)00356-6](https://doi.org/10.1016/S0377-0273(02)00356-6)
 48. K. A. Horton, G. Williams-Jones, H. Garbeil, T. Elias, A. J. Sutton, P. Mougins-Mark, J. N. Porter, S. Clegg, Real-time measurement of volcanic SO₂ emissions: Validation of a new UV correlation spectrometer (FLYSPEC). *Bull. Volcanol.* **68**, 323–327 (2006). [doi:10.1007/s00445-005-0014-9](https://doi.org/10.1007/s00445-005-0014-9)
 49. R. E. Stoiber, L. L. Malinconico, S. N. Williams, "Use of the correlation spectrometer at volcanoes," in *Forecasting Volcanic Events*, H. Tazieff, J. C. Sabroux, Eds. (Elsevier, 1983), pp. 424–444.
 50. G. Williams-Jones, J. Stix, P. A. Nadeau, "Using the COSPEC in the field," in *The COSPEC Cookbook: Making SO₂ Measurements at Active Volcanoes*, G. Williams-Jones, J. Stix, C. Hickson, Eds. (Special Publications of IAVCEI, IAVCEI, 2007), pp. 63–119.
 51. Y. Okada, Surface deformation due to shear and tensile faults in a half-space. *Bull. Seismol. Soc. Am.* **75**, 1135–1154 (1985).

ACKNOWLEDGMENTS

Any use of trade, firm, or product names is for descriptive purposes only and does not imply endorsement by the U.S. Government. Some work was carried out under research permit from Hawaii Volcanoes National Park. The authors appreciated thorough comments from M.T. Mangan and D. Dzurisin. **Funding:** Part of this research was carried out at the Jet Propulsion Laboratory, California Institute of Technology, under a contract with the National Aeronautics and Space Administration. **Author contributions:** C.A.N. and S.R.B. managed the eruption response and contributed to writing. E.K.M. produced the geodetic models, timeline figure and coordinated writing of the manuscript. B.S. contributed the seismic analysis and contributed to writing. H.R.D. contributed the lava flow models and contributed to writing. K.R.A. produced the DEM and cross section figure, supplementary caldera collapse movie and contributed to writing. P.A.N. and C.K. analyzed gas data and contributed to writing. R.L.L. and C.G. contributed petrology analysis. P.L. processed the ALOS-2 interferograms. J.B. and M.H.Z. compiled GIS data and produced the lava flow map. J.L.B. contributed to media organization and writing. A.K.D. processed the DEMs and collected, processed and managed the UAS data and contributed to writing. I.A.J. and A.M. collected and processed the geodetic data and contributed to writing. M.P. and C.P. collected and analyzed geologic data. W.A.T. contributed to seismic analysis and conceptualized the manuscript. M.B., P.D., and J.C. contributed to seismic analysis. All other authors contributed to the eruption response or writing of the manuscript. **Competing interests:** The authors declare no competing interests. **Data and materials availability:** Data access information and additional methodologies are provided in the manuscript or supplementary material and in these references: geologic data (16, 39), seismic data (40, 41), geodetic data (42, 43), and digital elevation data (44, 45).

SUPPLEMENTARY MATERIALS

www.sciencemag.org/cgi/content/full/science.aav7046/DC1

Materials and Methods

Figs. S1 and S2

References (47–57)

Movies S1 and S2

11 October 2018; accepted 3 December 2018
Published online 11 December 2018
10.1126/science.aav7046

Downloaded from <http://science.sciencemag.org/> on December 19, 2018

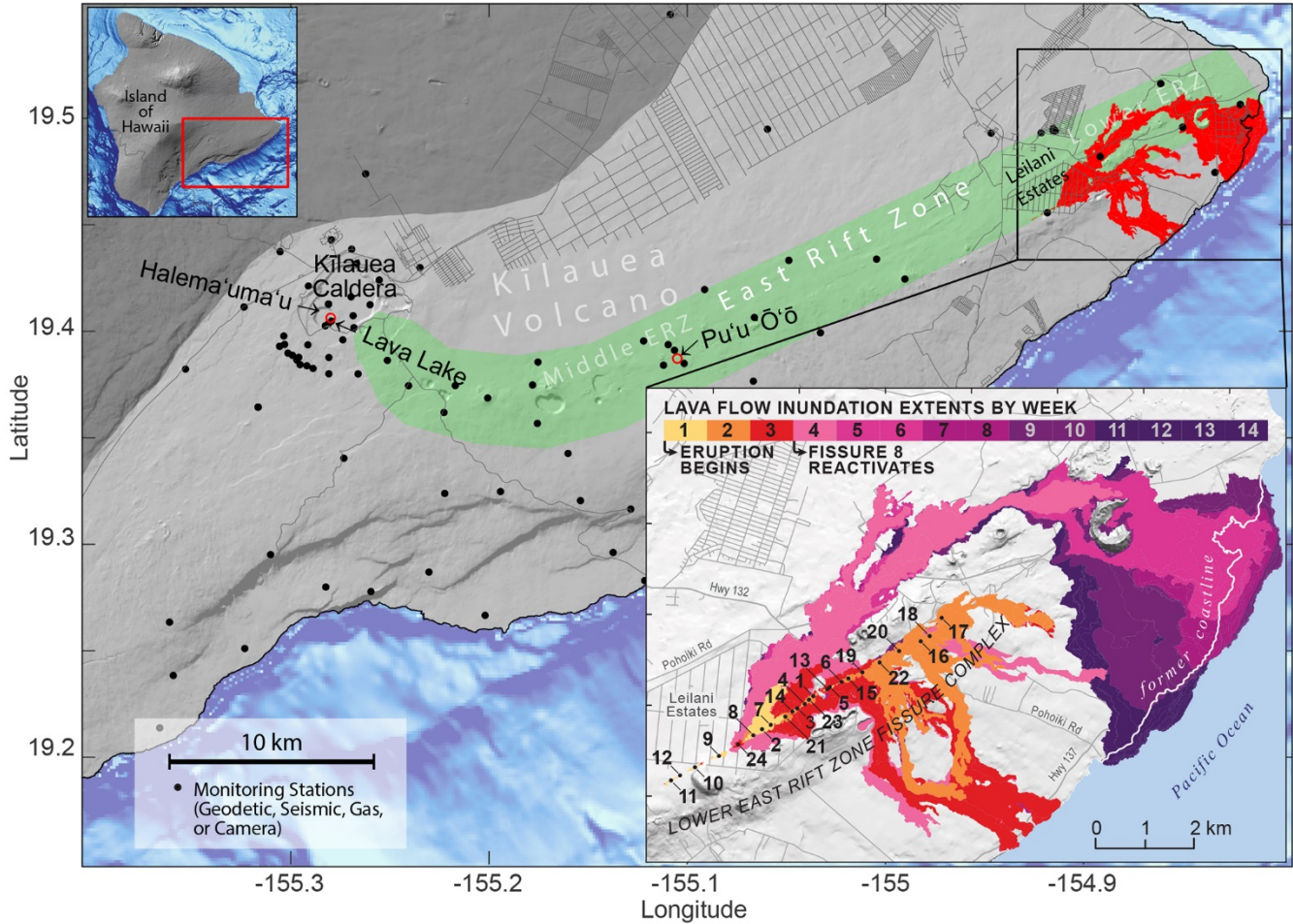


Fig. 1. Map showing the location of Kilauea Volcano on the Island of Hawai'i and the general geographic features of the volcano. The Kilauea Volcano is indicated in light gray. Black lines are roads and dots mark the locations of monitoring stations (geodetic, seismic, gas or camera). Locations of summit and Pu'u 'Ō'ō eruptive vents given by red circles. Green area indicates East Rift Zone. (Inset) Map of LERZ lava flows (39) with colors indicating the week during which a particular part of the flow was active. The labels 1-24 indicate eruptive fissure locations numbered according to the order of their formation.

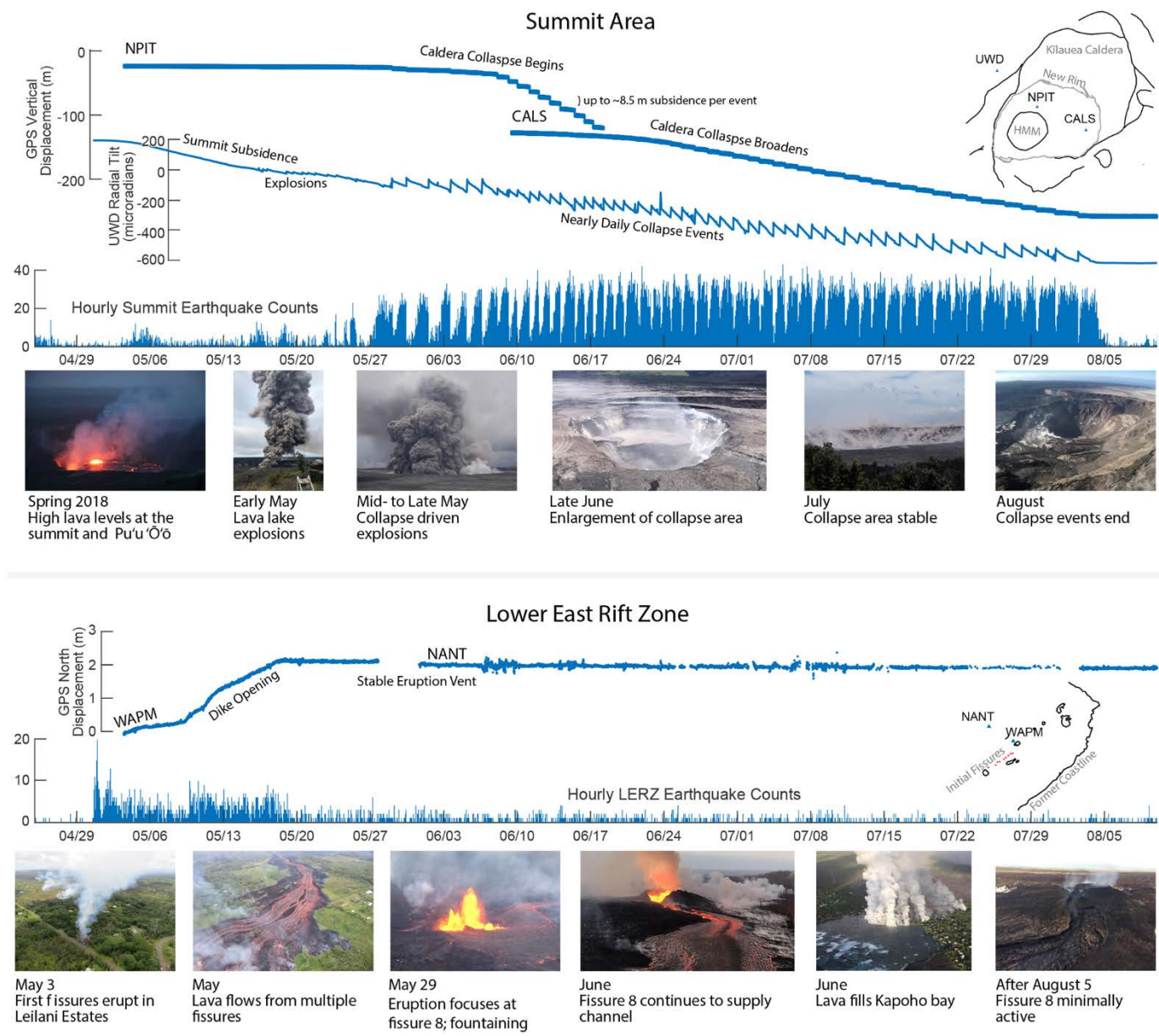


Fig. 2. Timeline of Kilauea's 2018 eruptive activity with representative geodetic and seismic data. (Top) Activity in the summit area of Kilauea through the time series of GNSS sites located near the initial focus of collapse (NPIT) and farther away (CALs). Nearly daily collapse events are manifested as spikes on the UWD tiltmeter and in hourly summit-area earthquake counts. **(Bottom)** Lower East Rift Zone activity, where deformation was observed by two GNSS sites (WAPM and NANT) on the north side of the fissures. The initial intrusion produced over 2 m of northward displacement at WAPM and coincided with substantial seismicity. After a swarm of about 100 earthquakes at Pu'u Ō'ō on 30 April to 1 May, middle East Rift Zone seismicity rates were around 1-2 events per hour, much less than the summit and LERZ.

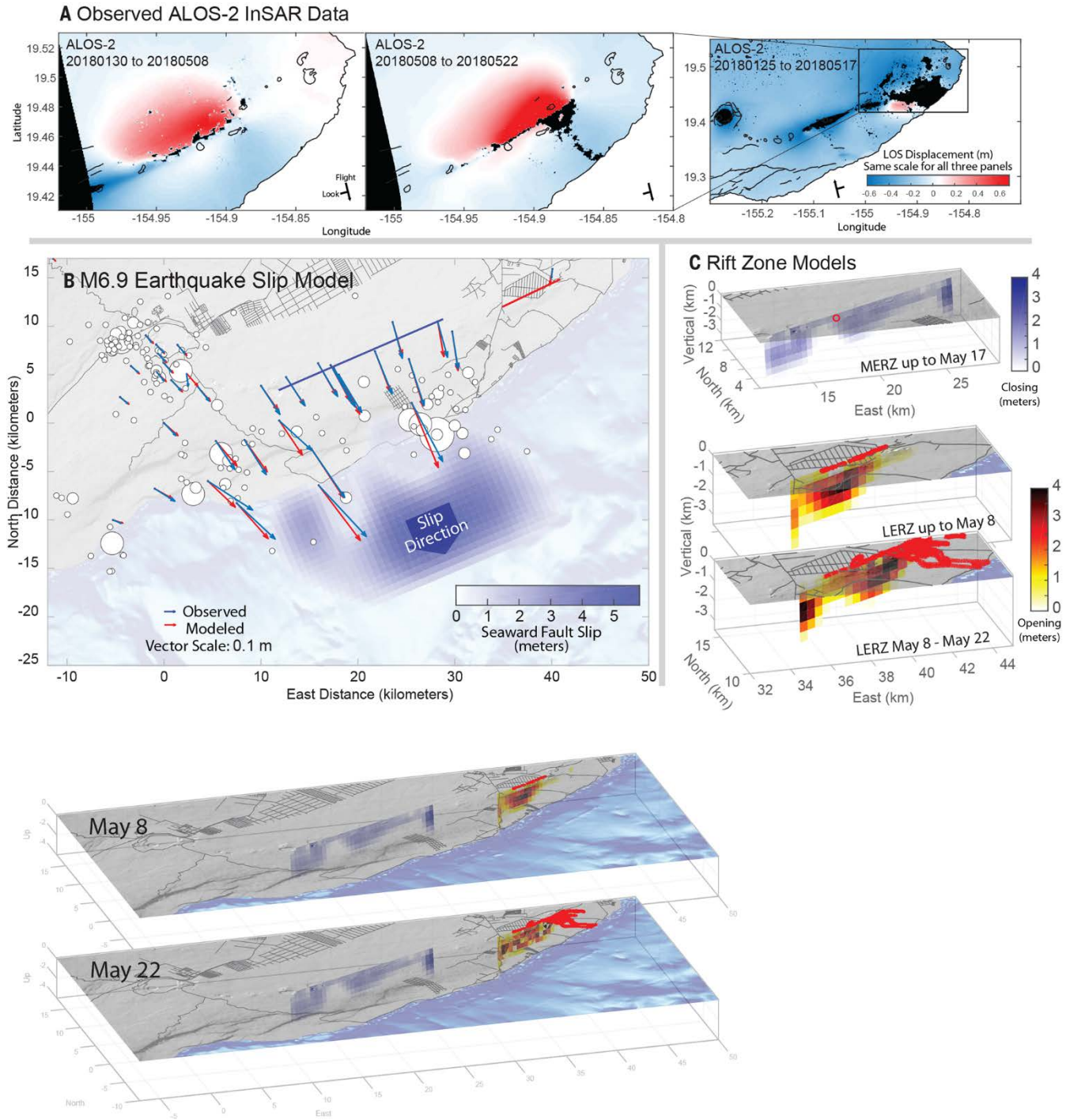


Fig. 3. Surface deformation and models of 2018 eruptive and earthquake activity. (A) Example InSAR line-of-sight displacement data from the ALOS-2 satellite used during the eruption (scale bar is the same for all three images). (B) GNSS displacements and model of the May 4 M6.9 earthquake (vector uncertainties are smaller than the arrowheads). (C) Example models of rift zone deformation utilizing the ALOS-2 data in (A). The top model shows a cross section along the blue line in (B), while the sections covered by the lower two models is shown by the red line in (B). In the models, fault slip and rift zone deformation are represented by simple elastic half-space solutions and were produced following previously published inversion methodologies [(46), fig. S1].

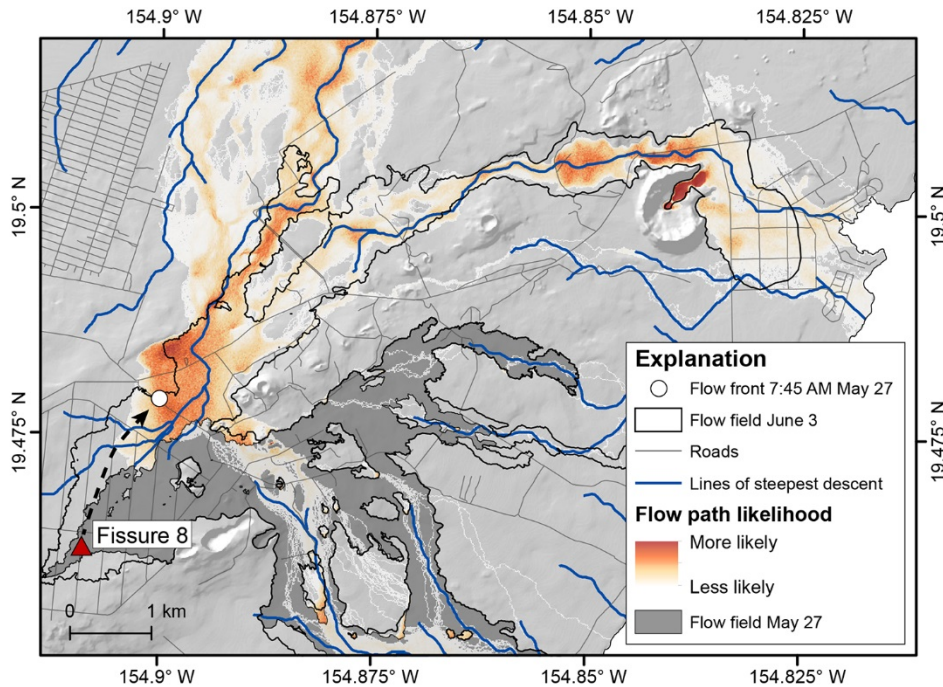


Fig. 4. Example lava flow forecast map. Initial lava flow path forecast for the Fissure 8 flow on May 27 (warm colors) compared to the mapped flow extent on June 3 (black outline) and pre-eruptive lines of steepest descent [blue lines; (16)]. Potential flow paths were simulated with DOWNFLOW (17) from approximate flow front positions reported by field crews (in this case, at the flow margin on the road, rather than the true inaccessible flow front further east) and pre-eruptive topography updated within the extent of new flows. Resulting maps were preliminary for operational use, and produced on-demand as the flows progressed following on decades of syn-eruptive flow mapping and expanding the past use of steepest descent paths for flow modeling.

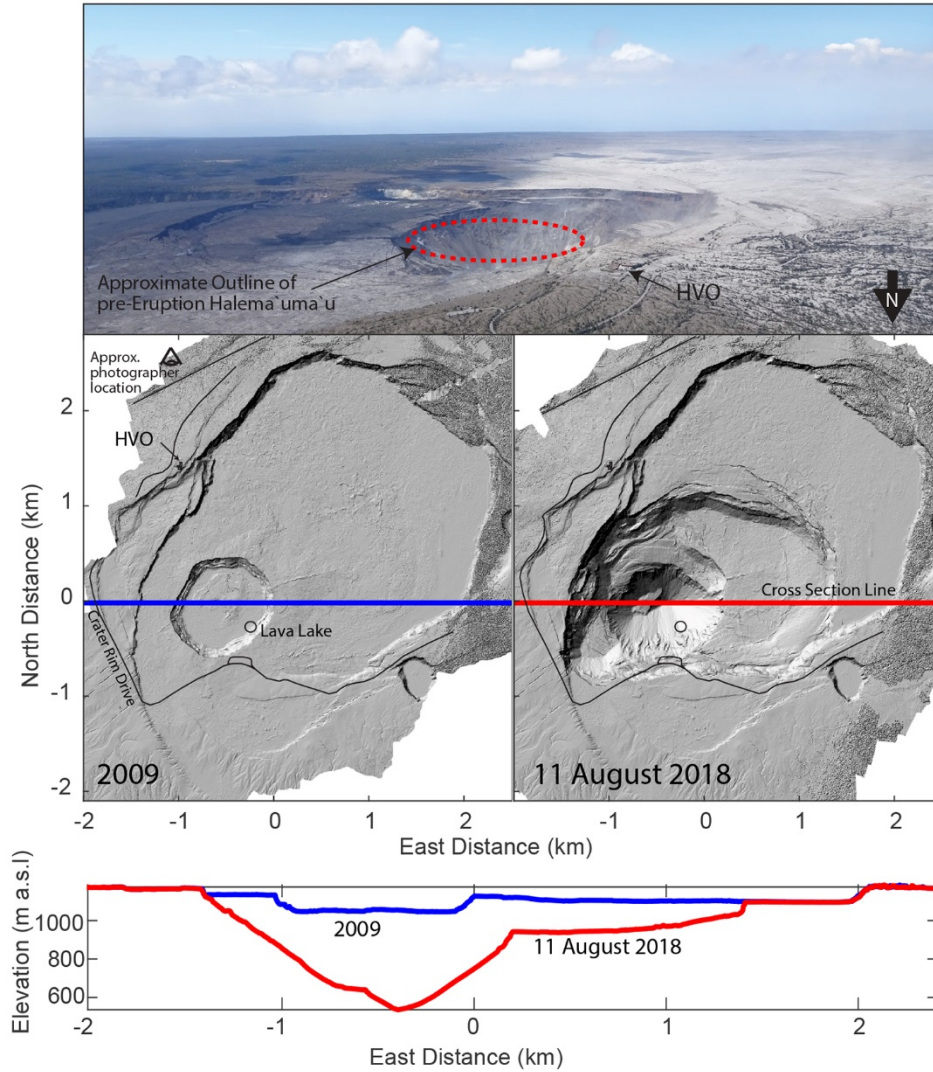


Fig. 5. Digital elevation changes at the summit of Kilauea Volcano. Lidar Digital Elevation Models of Kilauea's summit from 2009 (left) and 11 August, 2018 (right) showing the collapse of the caldera. Black lines indicate roads; the locations of the Hawaiian Volcano Observatory (HVO) and former lava lake are indicated. The red and blue lines correspond to the locations of the cross sections below. The difference between 2009 and 2018 topographic profiles gives the amount of subsidence that occurred almost entirely since 1 May 2018. Photo at top was taken NW of the caldera looking to the SE after the collapse.

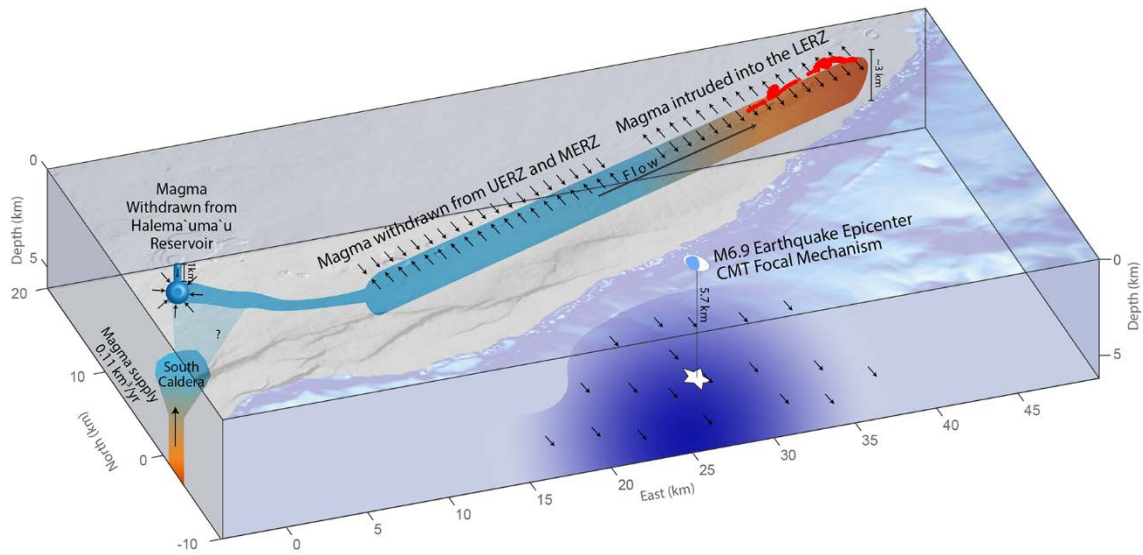


Fig. 6. Schematic representation of the subsurface redistribution of magma during the 2018 Kilauea eruptions. Orange colors depict areas that inflated, while turquoise indicate areas from which magma was withdrawn.

The 2018 rift eruption and summit collapse of Kilauea Volcano

C. A. Neal, S.R. Brantley, L. Antolik, J. Babb, M. Burgess, K. Calles, M. Cappos, J. C. Chang, S. Conway, L. Desmither, P. Dotray, T. Elias, P. Fukunaga, S. Fuke, I. A. Johanson, K. Kamibayashi, J. Kauahikaua, R. L. Lee, S. Pekalib, A. Miklius, W. Million, C. J. Moniz, P. A. Nadeau, P. Okubo, C. Parcheta, M. P. Patrick, B. Shiro, D. A. Swanson, W. Tollett, F. Trusdell, E. F. Younger, M. H. Zoeller, E. K. Montgomery-Brown, K. R. Anderson, M. P. Poland, J. Ball, J. Bard, M. Coombs, H. R. Dieterich, C. Kern, W. A. Thelen, P. F. Cervelli, T. Orr, B. F. Houghton, C. Gansecki, R. Hazlett, P. Lundgren, A. K. Diefenbach, A. H. Lerner, G. Waite, P. Kelly, L. Clor, C. Werner, K. Mulliken and G. Fisher

published online December 11, 2018

ARTICLE TOOLS

<http://science.sciencemag.org/content/early/2018/12/10/science.aav7046>

SUPPLEMENTARY MATERIALS

<http://science.sciencemag.org/content/suppl/2018/12/10/science.aav7046.DC1>

REFERENCES

This article cites 28 articles, 8 of which you can access for free
<http://science.sciencemag.org/content/early/2018/12/10/science.aav7046#BIBL>

PERMISSIONS

<http://www.sciencemag.org/help/reprints-and-permissions>

Use of this article is subject to the [Terms of Service](#)